NEW METHOD OF INVESTIGATION OF SINGULARITIES OF FEYNMAN DIAGRAMS

A. P. RUDIK and Yu. A. SIMONOV

Institute of Theoretical and Experimental Physics

Submitted to JETP editor April 3, 1963

J. Exptl. Theoret. Phys. (U.S.S.R.) **45**, 1016-1029 (October, 1963)

A new method is proposed for the determination of singularities of Feynman diagrams. The essence of the method consists in breaking up the diagram into separate blocks whose singularities are assumed known. An equation is obtained expressing the singularities of the diagram as a whole in terms of the singularities of the individual blocks. For a number of diagrams the singularities were found by the new method as well as by the Landau method. In particular, it is shown that the complex singularities that have been erroneously found previously by Kim[16] do not exist.

1. INTRODUCTION

AT this time the analytic properties of the amplitudes of quantum field theory are always postulated. This in particular is true of the Mandelstam representation.[1] Numerous attempts[2] of deriving the Mandelstam representation in the framework of perturbation theory have so far been unsuccessful. This is connected, in part, with the fact that so far we know only very poorly the analytic properties of the amplitudes even in perturbation theory. In fact, relatively detailed analysis of singularities of only the three simplest diagrams of perturbation theory exists (Figs. 1—3 and also the triangle diagram, Fig. 4b).

As has been shown by Karplus et al,[3] for the diagram of Fig. 1 there may arise anomalous thresholds and complex singularities for sufficiently large external masses. For diagrams of Fig. 2 Eden et al[4] have shown that for values of external masses for which anomalous singularities are yet absent the singularity curves have isolated singular points and become self-intersecting. The same is true of the diagram of Fig. 3,[5] but for it in addition there may arise anomalous asymptotes to the singularity curves under conditions when the external masses are not anomalous,[6] i.e., each of the mentioned diagrams has singular curves with its own peculiar properties. Therefore, the attempts at the study of more complicated diagrams are fully justified; the hope being that new substantial characteristics of analytic properties of the amplitudes might be obtained.

These attempts usually make use of one of two general approaches. In the first place one has the Landau method[7] for the study of the singular

FIG. 1   FIG. 2   FIG. 3

curves of arbitrary diagrams. This method makes it possible to determine all singularities that arise for real values of the Feynman parameters (and consequently for real values of the energy invariants) on the physical sheet.

Supported by the work of Cutkosky[8] and Polkinghorne and Screaton[9] the Landau method makes it possible to determine the complex singularities as well. However, then the analysis of the existence of the singularities on the physical sheet become substantially more complicated. Apparently the Landau method makes it possible to determine all the singularities of the diagram on the physical sheet. In any event, all the singularities on the physical sheet that have been found so far are obtainable by this method. In practice, however, for sufficiently complicated diagrams the Landau method also becomes too complicated in that it is very lengthy and requires for each diagram the solution of systems of algebraic equation that may require special approaches.

The second approach is related to the use of the unitarity relation and makes it possible to obtain the singularity curves for a number of diagrams in a very simple form without solving any systems of algebraic equations. However, this method is simple only if the unitarity relation is two-particle (for example for the diagram of Fig. 1) and becomes substantially more complicated if there appear three particles in intermediate states (the analysis of the unitarity relation for the diagram of Fig. 2 has been carried out by Gribov and Dyatlov

[10]). Moreover if the diagram contains both two-particle and three-particle intermediate states then compensation of singularities arising in the corresponding absorptive parts is possible.[11]

The method proposed by us, which we shall call in the following "block method," can be applied to a sufficiently large class of diagrams. With its help one obtains equations for the singularities immediately in a very simple form and, in contrast to the second method, without requiring tedious analysis. Moreover this method makes it possible to obtain all the singularities of the diagram and not only those of the absorptive parts, and the difficulty connected with the compensation of singularities does not arise.

This method also differs conveniently from the Landau method in its simplicity since there is no need to solve rather complicated systems of algebraic equations that arise in the Landau method. This simplicity will become particularly clear when we compare the operations in Secs. 2 and 3.

The approach proposed here for the study of the singularities of the diagrams may also be utilized for the calculation of the absorptive parts and of the spectral functions $\rho(s,t)$ of the Mandelstam representation (respectively of the kernel in the Bergmann-Weil representation when the Mandelstam representation is violated). A separate article of the authors is devoted to these questions.

In Sec. 2 the block method is applied to the study of the singularities of the diagrams shown in Figs. 4—7. At the end of the chapter we formulate general rules for the finding of the singularities of diagrams of a certain class (Fig. 8). In Sec. 3 the singular curves for the diagrams of Figs. 4 and 5 are obtained by the Landau method. Naturally, the results agree with the results of Sec. 2. In conclusion we discuss the results.

2. THE BLOCK METHOD OF STUDY OF DIAGRAM SINGULARITIES

In this section we shall consider a new method for the investigation of singularities of diagrams on the example of the diagrams shown in Figs. 4—8. In principle, this methods makes it possible to obtain all the singularities of the diagram on the physical sheet and also (with appropriate changes) on other sheets of the Riemann surface. First we shall find the equations for the singularities of the diagrams 4—7 without indicating on what sheet these singularities lie, that is we obtain the necessary conditions for the singularities. Sufficient conditions may be formulated in a simple form and
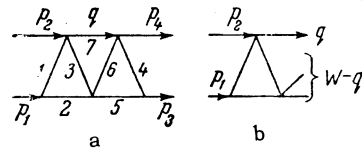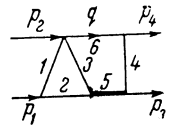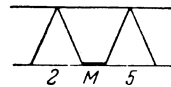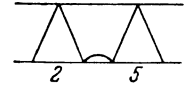

FIG. 4

FIG. 5

FIG. 6

FIG. 7

this will be done at the end of this chapter. Making use of these conditions we determine all the singularities of the diagrams of Figs. 1—4.

We write the Feynman integral for the diagram of Fig. 4a. At that we take into account that the right and left parts of it represent by themselves triangle diagrams, i.e., we assume that the integration over the virtual momentum in the contours of the triangle diagrams 1, 2, 3, and 4, 5, 6 has already been carried out. Then the amplitude corresponding to the diagram of Fig. 4a may be written in the form (ignoring unimportant factors)

$$A(s,t)$$
$$= \int \frac{B[m_1^2, (q-W)^2, (p_2-q)^2] B[m_2^2, (q-W)^2 (p_4-q)^2]}{q^2 - m^2 + i\varepsilon} d^4q. \tag{1}$$

Here $s = (p_1 + p_2)^2$, $t = (p_2 - p_4)^2$, $W = p_1 + p_2$.

To begin with we assume for simplicity that all the masses are the same and equal to m, and then we shall consider the case for anomalous masses for the particles p_1 and p_3: $M^2 > 2m^2$. $B(u_1, u_2, u_3)$ is the amplitude corresponding to the triangle diagram formed by the lines 1, 2, 3 (respectively 4, 5, 6) in Fig. 4b. We know its analytic properties as a function of the complex variables u_1, u_2, u_3 (see, for example,[12-14]) and it is therefore convenient to pass from integration over components of the vector q to integration over the energy invariants including u_1, u_2, u_3.

This may be done in the following manner: Let us write

$$d^4q = \tfrac{1}{2} dq_0 d\mathbf{q}^2 |\mathbf{q}| d\varphi d\cos\vartheta.$$

$d\varphi d\cos\vartheta$ may be rewritten in the well known manner:[10,15]

$$d\varphi d\cos\vartheta = dz_1 dz_2 / \sqrt{-K(z, z_1, z_2)}. \tag{2}$$

Here z stands for the cosine of the scattering angle, i.e., the angle between the vectors p_2 and p_4, $z = 1 + 2t/(s - 4m^2)$; z_1 is the cosine of the angle between the vectors p_2 and q; z_2 is the cosine of the angle between the vectors p_4 and q. The integration is carried out over a region in which $-K(z, z_1, z_2) > 0$, i.e., for example over
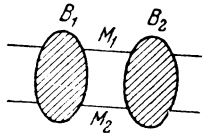
FIG. 8

FIG. 9   FIG. 10

dz_2 between the zeros of the function K and over dz_1 between -1 and $+1$. The function K has the form

$$K(z, z_1, z_2) = z^2 + z_1^2 + z_2^2 - 2zz_1z_2 - 1.$$

We go over from integration over dq_0 and dq^2 to integration over the variables q^2 and $\alpha = (W - q)^2$. Let us consider for simplicity the center-of-mass system of the vectors p_1 and p_2. Then

$$\alpha \equiv (W - q)^2 = q^2 - 2q_0\sqrt{s} + s,$$

$$q_0 = (q^2 + s - \alpha)/2\sqrt{s},$$

$$\mathbf{q}^2 = q_0^2 - q^2 = [(s + q^2 - \alpha)^2 - 4sq^2]/4s,$$

$$dq_0 d\mathbf{q}^2 = \tfrac{1}{2} s^{-1/2} dq^2 d\alpha. \tag{3}$$

The integration was carried out between the limits $(-\infty, \infty)$, over dq_0 and between the limits $(0, \infty)$ over $d\mathbf{q}^2$. The limits of integration over $d\alpha$ for fixed q^2 are determined from the condition of positiveness of $\mathbf{q}^2(\alpha)$, i.e., for $q^2 > 0$ and $s > 0$ we obtain $\alpha < \alpha_-$ and $\alpha > \alpha_+$, where

$$\alpha_\pm = (\sqrt{s} - \sqrt{q^2})^2. \tag{4}$$

The contours of integration $C(q^2)$ are shown in Fig. 9. For $q^2 < 0$ the region of integration encloses the entire real axis. The integration over dq^2 is carried out from $-\infty$ to $+\infty$. to $+\infty$.

Let us introduce the symbols $t_1 \equiv (p_2 - q)^2$ and $t_2 \equiv (p_4 - q)^2$. The quantities z_1 and z_2 are expressed in terms of these new variables as follows:

$$z_{1,2} = [2t_{1,2} - 2m^2 - q^2 + s - \alpha]/4pk(\alpha). \tag{5}$$

Here $k(\alpha) \equiv |\mathbf{q}(\alpha)|$ and is determined by Eq. (3), $p = \tfrac{1}{2}\sqrt{s - 4m^2}$.

$A(s,t)$ can be rewritten in the following form (again omitting unimportant factors):

$$A(s, t) = \int_{-\infty}^{\infty} \frac{dq^2}{q^2 - m^2 + i\varepsilon} \int_{C(q^2)} d\alpha k(\alpha) \int \frac{dz_1 dz_2}{\sqrt{-K(z, z_1, z_2)}}$$

$$\times B(m^2, \alpha, t_1) B(m^2, \alpha, t_2). \tag{6}$$

Let us consider the singularities of the functions $B(m^2, \alpha, t_i)$ (the form of the functions B is unimportant as long as we know their singularities). That is

$$\alpha = 4m^2, \quad t_i = t_i^m = 4m^2,$$

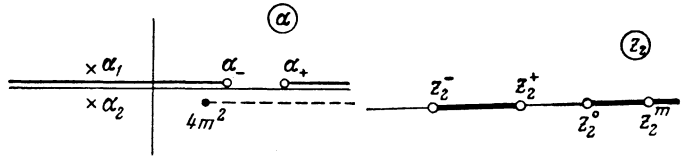$$t_i = t_0(\alpha) = m^2 + \alpha/2 + \tfrac{1}{2}\sqrt{3\alpha(4m^2 - \alpha)}. \tag{7}$$

The last singularity in t_i arises when α lies inside a hyperbola that crosses the real axis at the point $\alpha = 3m^2$ and is oriented towards $\alpha = +\infty$ [13,14], i.e., for real α this singularity arises for $\alpha \ge 3m^2$. For $\alpha > 4m^2$ the root in (7) must be understood as $-i\sqrt{3\alpha(4m^2 - \alpha)}/4$.

Let us consider the last integral in the expression (6):

$$\chi(\alpha, q^2, z, z_1, s) = \int_{z_2^-}^{z_2^+} \frac{dz_2 B(m^2, \alpha, t_2)}{\sqrt{-K(z, z_1, z_2)}},$$

$$z_2^\pm = zz_1 \pm \sqrt{(1 - z^2)(1 - z_1^2)}. \tag{8}$$

The contour of integration and the singularities in z_2 of the function $B(m^2, \alpha, t_2)$ in the z_2 plane are shown in Fig. 10.

The point z_2^0 corresponds to $t_2 = t_0(\alpha)$ and is expressed in terms of it with the help of (5):

$$z_2^0 = [s - q^2 + \sqrt{3\alpha(4m^2 - \alpha)}]/4pk(\alpha); \tag{9}$$

z_2^m is related in an analogous fashion to $t_2 = 4m^2$.

The singularity of the function χ arises when one of the ends of the contour of integration $z_2^\pm$ coincides with z_2^0 or z_2^m. The proper Landau singularity of the diagram of Fig. 4a corresponds to the case when $z_2^\pm$ coincides with z_2^0. The second case will be considered below. Making use of Eq. (8) we find for χ a singularity when

$$z_1 = z_1^\pm = zz_2^0 \pm \sqrt{(1 - z^2)[1 - (z_2^0)^2]}. \tag{10}$$

The integral over dz_1 can be rewritten in the form

$$\varphi(\alpha, q^2, s, t) = \int_{-1}^{1} dz_1 B(m^2, \alpha, t_1) \chi(\alpha, q^2, z, z_1, s).$$

The contour of integration and the singularities of the functions B and χ are shown in Fig. 11. For $z_2^0 > 1$ and $z < 1$ the points $z_1^\pm$ lie in the complex plane, for $z = 1$ they reach the real axis and move apart: z_1^+ goes to the right whereas z_1^- for $z = z_2^0$
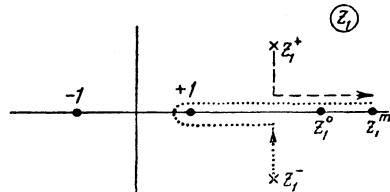

FIG. 11

goes around the contour of integration at the point $z_1 = +1$ and again goes off to the right. A singularity of the function φ arises when after surrounding the contour z_1^- coincides with z_1^0 or with z_1^m. Let us first consider, as above, the first case.

Thus the singularity of the function $\varphi(\alpha, q^2, s, t)$ has the form $z_1^- = z_1^0$ or $z = z_1^0 z_2^0 + \sqrt{[(z_1^0)^2 - 1][(z_2^0)^2 - 1]}$. In our case, when the masses are equal, $z_1^0 = z_2^0$ and

$$z = 2(z_1^0)^2 - 1, \tag{11}$$

where z_1^0 depends on α, q^2, and s.

It remains to consider the integrals over dq^2 and over $d\alpha$. It is clear from the form of the integral over dq^2 that the singularities of the function $A(s, t)$ arise when $q^2 = m$ (other cases correspond to singularities of diagrams obtained from the diagram of Fig. 4a by contracting the lines with q; for the moment we are not interested in these). A more detailed analysis of the condition for simultaneous pinching of contours over q^2 and α will be carried out below.

Consequently, if we set $q^2 = m^2$ we should consider the integral

$$A(s, t) \sim \int_{C_\alpha} d\alpha k(\alpha) \varphi(\alpha, s, t). \tag{12}$$

The singularities of the function $\varphi(\alpha, s, t)$ are given by Eq. (11), which we shall write in the form

$$F(\alpha, s, t) = 0, \tag{13}$$

and, in addition, by $\alpha = 4m^2$ which corresponds to the singularity $B(\alpha)$. The function $k(\alpha)$ has singularities for $\alpha = \alpha_-$ and $\alpha = \alpha_+$, i.e., at the edges of the contour of integration, independently of s. The singularity $A(s, t)$ arises, for the first time, when the point α_- coincides with the point $\alpha = 4m^2$ (the relative positions of α_- and $4m^2$ on Fig. 9 are given with the imaginary additions to the masses taken into account $m^2 \rightarrow m^2 - i\epsilon$).

This gives us $s = 9m^2$ and corresponds to the threshold of the three-particle state (cut through its diagram of Fig. 4a across lines 2, 3, and 7 or 5, 6, and 7). The coincidence of the point α_- and the singularity (13) does not occur for any finite t since $k(\alpha)$ for $\alpha = \alpha_-$ vanishes, and z_1^0 contains $k(\alpha)$ in the denominator, so that the singularity $A(s, t)$ can arise only for t strictly equal to infinity.

Equation (13) for fixed s and t gives several points α_i, at which $\varphi(\alpha, s, t)$ has singularities. In our case the Eq. (13) is of fourth order in α and therefore there are four such points. The singularity $A(s, t)$ may arise if any of the points α_i, for example α_1 and α_2, pinch the contour of integration over $d\alpha$. It is easy to see that the condition for the coincidence of the roots of Eq. (13) is of the form

$$\partial F(\alpha, s, t)/\partial \alpha = 0. \tag{14}$$

Equations (13) and (14) constitute a one-parameter set of equations for the determination of the singularities of the diagram of Fig. 4a. This set coincides with the corresponding set of Landau equations, in which all Feynman parameters α_i have been excluded except for a certain combination of them (see next Section).

If Eq. (14) can be solved for α as a function of s and t, then substitution of that value into Eq. (13) gives the equation for the singularities $\Phi(s, t) = 0$. In our case, however, Eq. (14) is of fourth degree with respect to α and such a procedure is, apparently, nonsensical.

We study the system of Eqs. (13) and (14) for s close to $9m^2$. Let $s = 9m^2 + \epsilon$. Equation (14) yields four values α_i: $\alpha_1 = 4m^2 - \epsilon^2/12$, another real value between α_- and α_+, and two values in the complex plane. Pinching of the integration contour occurs only for the value $\alpha = \alpha_1$, at that when $\epsilon > 0$ then $\alpha_- > 4m^2$, $\alpha_1 < 4m^2$ and pinching occurs, whereas when $\epsilon < 0$ then $\alpha_1 > \alpha_-$ and the coincidence of the roots occurs outside the contour of integration giving no singularity. Consequently only that branch of the curve defined by Eqs. (13) and (14) is singular that passes through values $s \geq 9m^2$.

Substitution of $\alpha = 4m^2 - (s - 9m^2)^2/12$ into Eq. (13) gives the asymptotic form of the singular curve for the diagram of Fig. 1:

$$t = 72m^4 / (s - 9m^2) + 21m^2 + O(s - 9m^2). \tag{15}$$

By taking successive terms in the expansion in $s - 9m^2$, or directly from Eqs. (13) and (14), we find: a) that the singular curve is real in t for real s and vice versa, b) that the asymptotic expansion is in integer powers of $s - 9m^2$. For $s \rightarrow \infty$ the singular curve approaches asymptotically $t = 16m^2$ and lies entirely in the region $s \geq 9m^2$, $t \geq 16m^2$ (Fig. 12). Consequently the singular curve is included in the usual cuts $s = 9m^2 + r$, $0 \leq r < \infty$ and $t = 16m^2 + r'$, $0 \leq r' < \infty$, and
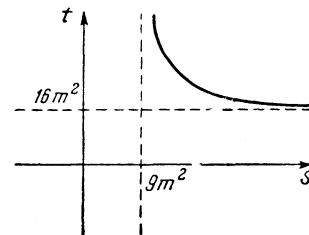

FIG. 12

therefore the function $A(s, t)$ has singularities only for real s and real t.[14] Therefore the Mandelstam representation is valid for the diagram of Fig. 1 and the region in which the spectral function fails to vanish is determined by the Eqs. (13) and (14).

These conclusions are in contradiction with those of Kim,[16] who found complex singularities by using three-particle unitarity without, however, carrying out a detailed analysis.

Before exploring the possible singularity of the diagram of Fig. 4, which occurs when the root α_1 of Eq. (13) coincides with $\alpha = 4m^2$, we discuss the diagram of Fig. 5, and establish the necessary conditions for the existence of singularities on the physical sheet. In our notation the amplitude $A(s, t)$ corresponding to the diagram of Fig. 5, may be written in the form

$$A(s, t) = \int_{-\infty}^{\infty} \frac{dq^2}{q^2 - m^2 + i\varepsilon} \int_{c_\alpha} \frac{d\alpha \varphi(\alpha, q^2, s, t)}{\alpha - M^2 + i\varepsilon}. \qquad (16)$$

In this case the sole difference from the preceding consists in the appearance of the pole in α, caused by line 5 with mass M, and also in the fact that $\varphi(\alpha, q^2, s, t)$ has a singularity for

$$z = z_1^0 z_2^m + \sqrt{[(z_1^0)^2 - 1][(z_2^m)^2 - 1]}, \qquad (17)$$

where z_2^m is defined by Eq. (5) with $t_2 = m^2$ (all masses are equal except for the mass on line 5, $m_5 = M$).

We write Eq. (17) as

$$F(\alpha, q^2, s, t) = 0. \qquad (18)$$

The proper singularity of the diagram of Fig. 5 corresponds to the case when the root in α of Eq. (17) coincides with M^2. If the root α_1 occupies the position shown in Fig. 13 then pinching of the contour of integration will occur and, consequently a singularity of the function $A(s, t)$. In that case the diagram of Fig. 5 would have complex singularities and the Mandelstam representation would be violated.

We introduce imaginary additions: $q^2 = m^2 - i\epsilon$ and $\alpha = M^2 - i\epsilon$ in order to clarify the question whether indeed a pinching of the contour occurs in the two consecutive integrations over $d\alpha$ and dq^2. We assume first that the contour of integration over $d\alpha$ is along the real axis. If $q^2 \rightarrow q^2 + i\epsilon_q$, $\alpha \rightarrow \alpha + i\epsilon_\alpha$, then the additions ϵ_q and ϵ_α are related, as a consequence of Eq. (18), by[1]

$$\varepsilon_\alpha \partial F/\partial \alpha + \varepsilon_q \partial F/\partial q^2 = 0. \qquad (19)$$

Pinching of the contour occurs if $\partial F/\partial \alpha$ and $\partial F/\partial q^2$ have the same sign. Indeed, in the opposite case for $\epsilon_q < 0$ we have from Eq. (19) $\epsilon_\alpha < 0$ and the contour is not pinched in the α plane, or, more precisely, for $\epsilon_q > 0$ the integral over α is an analytic function of q^2 in the upper half of the q^2 plane; the integral may be deformed in dq^2 into the upper half-plane and no singularity results.

In our case the contour of integration over $d\alpha$ and its end point α_- are functions of q^2: $\alpha_- = (\sqrt{s} - \sqrt{q^2})^2$. Let us take this circumstance into account. We set in Eq. (18) $\alpha = \alpha_- - \delta$, where δ is some real number so that α lies on the contour. Let $q^2 \rightarrow q^2 + i\epsilon_q$ and $\delta \rightarrow \delta - i\epsilon_\delta$. Then

$$\frac{\partial F}{\partial \alpha} \frac{d\alpha_-}{dq^2} \varepsilon_q + \frac{\partial F}{\partial \alpha} \varepsilon_\delta + \frac{\partial F}{\partial q^2} \varepsilon_q = 0; \qquad (20)$$

or

$$\varepsilon_q \delta F/\delta q^2 + \varepsilon_\delta \partial F/\partial \alpha = 0; \qquad \frac{\delta F}{\delta q^2} \equiv \frac{\partial F}{\partial \alpha} \frac{d\alpha_-}{dq^2} + \frac{\partial F}{\partial q^2}. \qquad (21)$$

The condition for the pinching of the contour now consists of the requirement that $\delta F/\delta q^2$ and $\partial F/\partial \alpha$ have the same sign. The critical moment occurs here when α_- goes past the point M^2, i.e., when $\alpha = M^2$ and s is such that δ is small. Making use of the explicit form of the function $F(\alpha, q^2, s, t)$ [Eq. (17)] we find that the signs of $\delta F/\delta q^2$ and $\partial F/\partial \alpha$ are different. This proves that the indicated complex singularity $F(M^2, m^2, s, t) = 0$ is absent from the physical sheet $M^2 = M^2 - i\epsilon$, $m^2 = m^2 - i\epsilon$.

By making use of the explicit form of $\delta F/\delta q^2$ and $\partial F/\partial \alpha$ one can establish that the point α_1 lies, for $\alpha_- < M^2$, above the contour and with increasing s, when $\alpha_- \rightarrow M^2$, passes the contour to the right and reaches the region below the contour of integration.

A similar analysis for the coincidence of the points α_1 and $\alpha = 4m^2$ for the diagram of Fig. 4a shows that α_1 and $\alpha = 4m^2$ lie on the same side of the contour of integration and no singularity results.

We turn next to the diagrams of Figs. 6 and 7. The expression for $A(s, t)$ has, as before, the form (16) in case of the diagram 6 except that $\varphi(\alpha, q^2, s, t)$ has a singularity of the form (11). The analysis of the positions of the singular points in accordance with Eq. (20) is even simpler this
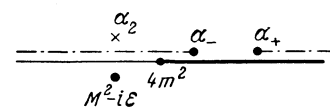
---

[1]This condition coincides with the equation considered by Drummond[17] in a different connection.

FIG. 13

time due to the simple form of Eq. (11). It shows that the singular points $\varphi(\alpha, q^2, s, t)$ and $M^2 - i\epsilon$ lie on the same side of the contour of integration and, consequently, the diagram, Fig. 6, has no proper singularities.

For the diagram of Fig. 7 the difference consists in the replacement of the pole term by a function (self-energy diagram) which has a branch point at $\alpha = 4m^2$. In this case, too, no pinching of the contour of integration over $d\alpha$ occurs and, consequently, the diagram of Fig. 7 has no proper singularities.

Before discussing the remaining singularities of the diagrams of Figs. 4—7, we introduce certain definitions.

A. We say that the diagram has a singularity of type A if the singularity-determining equation depends on one variable (normal and anomalous thresholds belong here).

B. A singularity of type B is described by Eq. (17), in which α was fixed. It arises due to coincidence of the singularities of the function $\varphi(\alpha, q^2, s, t)$ in Eq. (16) with the singularity for fixed α (for example, $\alpha = M^2 - i\epsilon$) at different ends of the contour of integration over $d\alpha$.

C. Singularities of type C are described by Eqs. (13) and (14) and are due to the coincidence of two singularities of the function $\varphi(\alpha, q^2, s, t)$.

The box diagram (Fig. 1) has only singularities of type A and B. The box diagram with a diagonal (Fig. 2) has singularities of type A and C.

The diagram of Fig. 4a has singularities of type A ($s = 9m^2$, $t = 16m^2$) and three singularities of type C. The first of these is the proper singularity of the given diagram, given by Eqs. (13)—(14). The two other singularities coincide if all internal masses are equal. They correspond to the case when we take into account in one of the triangle functions $B(m^2, \alpha, t_i)$ the singularity $z_i = z_i^m$ instead of $z_i = z_i^0$. Then we obtain instead of (13) and (14) the following equations for these singularities:

$$z - z_1^0 z_2^m - \sqrt{[(z_1^0)^2 - 1][(z_2^m)^2 - 1]} = 0,$$

$$\frac{\partial}{\partial \alpha}\{z - z_1^0 z_2^m - \sqrt{[(z_1^0)^2 - 1][(z_2^m)^2 - 1]}\} = 0, \quad (22)$$

where z_1^0 is defined in (9) and z_2^m is obtained from Eq. (5) when $t_2 = 4m^2$:

$$z_2^m = (s + 5m^2 - \alpha)/4pk\,(\alpha). \quad (23)$$

The singularity (22) is a singularity of the box diagram with the diagonal, Fig. 2, in which the right vertical line carries a double mass. We will not discuss here the character of this singularity, since the diagram of Fig. 2 has been investigated in detail

by Kolkunov et al[5] and Gribov and Dyatlov.[11]

The diagram of Fig. 5 has no proper singularities on the physical sheet and has singularities of type A ($s = 9m^2$, $s = (M+m)^2$, $t = 9m^2$) and of type B — the singularity of the box diagram on contraction of line 2, whose equation has the form

$$z = z_1^m z_2^m + \sqrt{[(z_1^m)^2 - 1][(z_2^m)^2 - 1]},$$

where z_1^m is defined by Eq. (23), α must everywhere be set equal to M^2, and

$$z_2^m = (s - m^2 - \alpha)/4pk(\alpha). \quad (23')$$

For the diagram of Fig. 5 a singularity of type C arises, as is easily seen, on contraction of line 5. This is the singularity of the box diagram with the diagonal. The singularity equation has the form (22) with z_2^m replaced by expression (23') instead of (23).

The diagrams of Figs. 7 and 8 have in addition to all the singularities of the diagram of Fig. 4a also singularities of type B corresponding to the box diagram (lines 2 and 5 contracted).

We consider now a diagram of the general type (Fig. 8) and formulate the rules for determining the singularities of the entire diagram if the singularities of the dashed-in parts are known. We denote these parts as certain functions $B_{1,2}(\alpha, q^2, s, t_{1,2})$. Then the singularities of type B are given by the equation $z = z_1 z_2 + \sqrt{(z_1^2 - 1)(z_2^2 - 1)}$, where $z_{1,2}$ are expressed with the help of Eq. (5) in terms of $t_{1,2}$ — the singular points of the functions $B_{1,2}$. In that equation it is necessary to set $\alpha = M_2^2$, $q^2 = M_1^2$.

The singularity of type C is given by the equations

$$z - z_1 z_2 - \sqrt{(z_1^2 - 1)(z_2^2 - 1)} = 0,$$

$$\frac{\partial}{\partial \alpha}[z - z_1 z_2 - \sqrt{(z_1^2 - 1)(z_2^2 - 1)}] = 0,$$

where $z_{1,2}$ are as before and $q^2 = M_1^2$. A second equation of type C results from the replacement $\alpha \rightleftharpoons q^2$.

An important and valuable property of the block method consists of the possibility of determining the singularities of the diagrams that were subsequently made more complicated (for example the diagrams shown in Fig. 14). Having determined the singularities of a certain diagram we may introduce it as a component part of a more complex diagram, in which it plays the role of the function $B_{1,2}$, and determine the singularities of this more complex diagram, etc.

Lastly we consider the case when the masses of particles p_2 and p_3 in the diagrams of Figs. 4—7 are anomalous, $M^2 > 2m^2$. Such diagrams
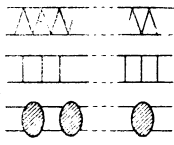
FIG. 14

FIG. 15

contribute, for example, to Nd scattering. One can show from Eqs. (13) and (14) that the singularity curve of the diagram, Fig. 4a, remains in the region $s \geq 9m^2$, $t \geq 16m^2$ and does not exhibit anomalous properties. Altogether no anomalous singularities arise for the diagram of Fig. 4a as a whole, and the diagrams of Figs. 5—7 have, as before, no proper singularities.

3. THE LANDAU METHOD

We consider now the singularities of the diagram, Fig. 4a, by the Landau method. The great advantage of this method lies in the comparative simplicity with which one can establish on what sheet the singular curve lies. In solving the set of Landau equations we make use of the method outlined in [5].

Since the masses of all the particles forming the diagram of Fig. 4a are assumed to be equal, there must exist among the solutions of the Landau equations a symmetric solution corresponding to the conditions $\alpha_1 = \alpha_4$, $\alpha_2 = \alpha_5$, $\alpha_3 = \alpha_6$. We shall start from a study of this case. We denote by q_{ik} the scalar products: $q_{ik} = q_i q_k$. From the symmetry conditions on α there follow symmetry conditions on the q_{ik}: $q_{37} = q_{67}$, $q_{16} = q_{34}$, $q_{13} = q_{46}$, $q_{23} = q_{56}$ (the last equality follows from the law of conservation of 4-momentum). Then s and t may be expressed in the form:

$$s = (q_7 + q_2 - q_3)^2 = 3 + 2q_{27} - 2q_{23} - 2q_{37},$$
$$t = (q_1 - q_3 + q_6 - q_4)^2 = 4 - 4q_{13} + 4q_{16} - 2q_{14} - 2q_{36}.$$
$$(24)$$

To establish a relation between the scalar products that enter the right-hand sides of Eqs. (24) we make use of Landau equations for the contours $\{1, 2, 3\}$ and $\{3, 7, 6\}$:

$$\alpha_1 q_1 + \alpha_2 q_2 + \alpha_3 q_3 = 0; \quad \alpha_3 (q_3 + q_6) + \alpha_7 q_7 = 0. \quad (25)$$

With the help of Eq. (25) and the conservation laws

$$1 = (q_1 + q_7 - q_3)^2 = 3 + 2q_{17} - 2q_{13} - 2q_{37},$$
$$q_{24} = q_{16} + q_{12} - q_{13} \quad (26)$$

it is easy to express q_{ik} in terms of the various α. Substituting these expressions in Eq. (24) we get (under the condition that $q_{12} = \frac{1}{2}$):

$$s = 3 + 4 \frac{\alpha_3}{\alpha_7} + 2 \frac{\alpha_1/2 + \alpha_2}{\alpha_3} \left(1 + \frac{2\alpha_3}{\alpha_7}\right),$$
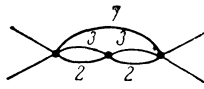
$$t = 6 + \frac{\alpha_2}{\alpha_1} - \frac{\alpha_7^2}{\alpha_3^2} + 2 \frac{\alpha_7}{\alpha_3} \left[1 + \frac{\alpha_7}{2\alpha_3} + \frac{\alpha_1 + \alpha_2/2}{\alpha_3}\right]$$
$$\times \left(2 + \frac{\alpha_2 + \alpha_3}{\alpha_1}\right) + 2 \frac{\alpha_1 + \alpha_2/2}{\alpha_3} \left[4 + \frac{\alpha_3 + 2\alpha_2}{\alpha_1}\right]. \quad (27)$$

It is next necessary to establish a relation between α_1, α_2, α_3, α_7. The trivial condition $\sum_{i=1}^{7} \alpha_i = 1$ provides one such relation; another is obtained by squaring the first of Eqs. (25), and a third follows from the Eqs. (25) and the conservation law $q_{26} = q_{36} + q_{23} - 1$:

$$2\alpha_1 + 2\alpha_2 + 2\alpha_3 + \alpha_7 = 1, \quad \alpha_3^2 = \alpha_1^2 + \alpha_2^2 + \alpha_1\alpha_2,$$
$$2\alpha_3 [(\alpha_2 + \alpha_3)^2 - \alpha_1^2] = \alpha_1\alpha_7 (1 - \alpha_2) + \alpha_7^2 (\alpha_2 + \alpha_3). \quad (28)$$

The four-parameter system (27)—(28) gives a singular curve $t = t(s)$. We consider the form of this curve when $t \to \infty$. It follows from Eq. (27) that the sole possibility of realizing $t \to \infty$ when $s \to \infty$ is the condition $\alpha_1 \to 0$. This condition is quite natural since then the diagram of Fig. 4a reduces to the diagram of Fig. 15.

We look for a solution for $\alpha_1 \to 0$ in the form of an expansion of α_2, α_3, and α_7 in powers of α_1. It is easily seen from the set of Eqs. (20) that this expansion must be in integer powers of α_1 only. After some simple manipulations we get

$$\alpha_2 = \frac{1}{6} [1 - \frac{5}{2} \alpha_1 - \frac{27}{4} \alpha_1^2], \quad \alpha_3 = \frac{1}{6} [1 + \frac{1}{2} \alpha_1 + \frac{27}{4} \alpha_1^2],$$
$$\alpha_7 = \frac{1}{3} (1 - 4\alpha_1). \quad (29)$$

As expected, the independent of α_1 terms in α_2, α_3, α_7 correspond to values of α_i in the reduced diagram, Fig. 15.

By substituting values for α_i (29) and expressions for s and t (27) we get

$$t = 4/\alpha_1 + 11, \quad s = 9 + 18\alpha_1 + 45\alpha_1^2 \quad (m = 1). \quad (30)$$

From Eq. (30) α_1 is easily expressible as a function of $(s - 9)$:

$$\alpha_1 = \frac{1}{18} (s - 9) [1 - \frac{5}{36} (s - 9)]. \quad (31)$$

Substituting α_1 from (31) into the expression for t from (30) we get the singular curve when $t \to \infty$:

$$t = 72/(s - 9) + 21 + O (s - 9). \quad (32)$$

This singular curve coincides with the curve (15) obtained in the preceding section. At that, as can be easily seen by transforming Eqs. (27)—(28), the agreement of the singular curves is not just asymptotic but constitutes an identity. It should be emphasized that the one-parameter connection (13)—(14) is obtained directly, whereas in the Landau method it follows after some rather difficult transformations of the system (28).

It follows from Eqs. (31) and (29) that for $s > 9$

all $\alpha > 0$ and the singular curve lies on the first sheet. For $s < 9$ $\alpha_1 < 0$ and the singular curve goes off to the second sheet. But it follows from Eqs. (27) and (28) that s and t are always given by real expressions, i.e., the symmetric case of Landau equations does not give rise to complex singularities.

We now analyze the question whether solutions exist to the Landau equations in the general case when the symmetry conditions are not imposed on the α_i. At that we make use of a slightly different parametrization of s and t: we express s and t in terms of the q_{ik} and not the α_i. Strictly speaking, in the nonsymmetric case we are forced to this type of parametrization because it is in principle impossible to determine all the α_i in the reduced diagram, Fig. 15, when $\alpha_5 \neq \alpha_2$ and $\alpha_6 \neq \alpha_3$. We also note that the parametrization of s and t by the q_{ik} makes it possible not to use the condition $\sum_i \alpha_i = 1$, $\alpha_i > 0$ and consequently investigate singularities of the second kind.[4,8]

Introducing the notation $X = q_{23} + q_{27}$ and $Y = q_{16} - q_{13}$ we obtain from the Landau equations and the conservation laws

$$s = 3 - 4q_{23} - 2q_{27} + 2X,$$

$$t = 4 (1 - q_{36}) (1 - q_{12}) (1 - q_{13})/(1 + q_{23}),$$

$$X = \frac{2 (1 - q_{23}^2)^{1/2} + (1 + q_{37}) [(1 - q_{12}^2)^{1/2} + (1 - q_{23}^2)^{1/2}]}{q_{23} (1 - q_{12}^2)^{1/2} + q_{12} (1 - q_{23}^2)^{1/2}}$$

$$= -\frac{q_{23} [(1 + q_{36}) (1 - q_{37}) + (1 - q_{36}^2)^{1/2} (1 - q_{37}^2)^{1/2}] + q_{67} - q_{36}q_{37}}{1 + q_{36}},$$

$$Y = (1 - q_{36}) \frac{(1 - q_{12}^2)^{1/2} (1 - q_{23}) - q_{12} (1 - q_{23}^2)^{1/2}}{(1 - q_{23}^2)^{1/2}}$$

$$= (1 - q_{36}) \frac{(1 - q_{13}) (1 - q_{37}) (1 + q_{36}) - q_{13} (1 - q_{36}^2)^{1/2} (1 - q_{37}^2)^{1/2}}{(1 - q_{36}^2)^{1/2} (1 - q_{37}^2)^{1/2}}.$$

$$(33)$$

We analyze now the system (33) in the asymptotic region $t \rightarrow \infty$ under the condition $q_{37} \neq q_{67}$ (the equality $q_{37} = q_{67}$ means passage to the symmetric case). It follows from Eqs. (33) that $t \rightarrow \infty$ either for $q_{23} \rightarrow -1$, or for $q_{36} \rightarrow -\infty$. Let $q_{23} = -1 + \eta^2/2$, where $\eta \ll 1$. Then in order that t $\rightarrow \infty$ when $\eta \rightarrow 0$ it is necessary that $1 - q_{36} \sim a\eta^\kappa$, where $\kappa < 2$. However this condition is in contradiction with the last of Eqs. (33).

A more complex situation arises when $q_{36} \rightarrow -\infty$. We confine ourselves in this case to the value $s = 9$. Introducing the notation $z = q_{67}/q_{36}|_{q_{36} \rightarrow \infty} = q_{37} - i(1 - q_{37}^2)^{1/2}$ we obtain from Eqs. (33)

$$iz^{7/2} + 7z^3 - iz^{5/2} + 9z^2 - 29iz^{3/2} - 15z - 3iz^{1/2} - 9 = 0,$$
$$- iz^{5/2} - 9z^2 + 16iz^{3/2} - 6z - 3iz^{1/2} - 9 = 0. \quad (34)$$

However Eqs. (34) have no common roots and therefore the case $q_{36} \rightarrow \infty$ cannot be realized. In this fashion, as a result of rather tedious operations, we arrive at the conclusion that in the nonsymmetric case the Landau equations for the diagram of Fig. 4a have no solutions when $t \rightarrow \infty$.

Equations (33) reduce easily to the symmetric case for $q_{37} = q_{67}$. In that case, naturally, one obtains the asymptotically singular curve (32).

To conclude this section we make a few remarks about the singular curves of the diagrams of Figs. 5 and 6. For their analysis it is convenient to use the method developed in [6], namely to reduce the problem of finding the singular curves of these diagrams to that of finding the singular curves of the effective diagram of Fig. 16, in which the external momenta, the masses and the α_i of the virtual particles 3 and 4 are related to the parameters of the original diagrams by

$$\alpha_3' = \alpha_3 \frac{(1 - q_{13}^2)^{1/2} + (1 - q_{23}^2)^{1/2}}{(1 - q_{12}^2)^{1/2} + (1 - q_{13}^2)^{1/2} + (1 - q_{23}^2)^{1/2}},$$

$$p_2' = p_2 + p_1 \frac{(1 - q_{13}^2)^{1/2}}{(1 - q_{13}^2)^{1/2} + (1 - q_{23}^2)^{1/2}},$$

$$p_1' = p_1 \frac{(1 - q_{23}^2)^{1/2}}{(1 - q_{13}^2)^{1/2} + (1 - q_{23}^2)^{1/2}}, \qquad m_3' = \frac{\alpha_3}{\alpha_3'}. \quad (35)$$

For the diagram of Fig. 5 the values of p_2' and p_4', as well as the values of the characteristics of the virtual particle 4' of the effective diagram, will coincide with the values in the original diagram, and for the diagram of Fig. 6 as a consequence of symmetry they will be expressed by formulas analogous to (35). This is, however, as far as we shall go in the study of these diagrams since the study of the diagram of Fig. 16, is in principle known albeit difficult (particularly in our case when the external masses of the effective diagram depend on the invariants of the original diagrams).

We also note that the diagram of Fig. 4a may be easily reduced to the diagram of Fig. 17 in which the quantities p_3', p_4', m_6', α_6' are defined in terms of the parameters of the original diagram of Fig. 4a as follows:

$$p_3' = \alpha_4 p_3 / (\alpha_4 + \alpha_5),$$

$$p_4' = p_4 + \alpha_5 p_3 / (\alpha_4 + \alpha_5);$$

$$\alpha_6' = (\alpha_4 + \alpha_5) \alpha_6 / (\alpha_4 + \alpha_5 + \alpha_6),$$

$$m_6' = (\alpha_4 + \alpha_5 + \alpha_6) / (\alpha_4 + \alpha_5). \quad (36)$$

We determine now the value of t' for the reduced diagram, Fig. 17 [it is obvious that the value of s is the same for the reduced diagram (Fig. 17) and the original diagram (Fig. 4a)]:

$$t' = (p_2 + p_4')^2 = \alpha_5^2/(\alpha_4 + \alpha_5)^2 + t\alpha_4/(\alpha_4 + \alpha_5), \quad (37)$$

where $t = (p_2 - p_4)^2$. We consider now the asymptotic value of the singular curve of the symmetric diagram Fig. 4a. As was explained at the beginning of this Section one has in that case $\alpha_4 = \alpha_1 \to 0$, $t \to 4/\alpha_1$. But it follows from Eq. (37) that for $t \to \infty$ $t' \to$ const, i.e., in order to find the asymptotic behavior of the singular curve of the diagram of Fig. 4a, one must study the singular curve of the nonsymmetric diagram, Fig. 17, ($m_3'^2 \neq 1$, $p_1^2 = p_2^2 \neq p_3'^2 \neq p_4'^2$) outside the asymptotic region, which by itself is a rather difficult task.

And, finally, a few words about the case when in the diagram of Fig. 4a $p_1^2 = p_3^2 = M^2 \neq 1$ (and all remaining masses are equal to unity). Let us make clear—in the symmetric case—whether such a diagram can have anomalous curves. To this end we use the fact that the value of the derivative dt/ds for the effective diagram of Fig. 17 is known.[18] We then have, using the expression for α_6' from Eq. (36)

$$dt/ds = -2\,\alpha_2\alpha_7\,(\alpha_1 + \alpha_2 + \alpha_3)/\alpha_1^2\alpha_3. \quad (38)$$

But it follows from Eq. (38) that $dt/ds = 0$ for $\alpha_2 = 0$ or $\alpha_7 = 0$, and $ds/dt = 0$ for $\alpha_1 = 0$ or $\alpha_3 = 0$. However the reduced diagrams obtained in these limits are of the form of triangle diagrams without anomalous thresholds. In this way we arrive at the conclusion that for $p_1^2 = p_3^2 = M^2 \neq 1$ the diagram of Fig. 4a has no anomalous singular curves.

4. CONCLUSION

In Sec. 2 we have shown that the "block" method makes it possible to write the singularity equation right away in the form of an equation connecting s and t, for singularities of type B; and in the form of a one-parameter system of equations for singularities of type C. The application of the block method is not limited to the case of equal internal masses, which was considered here only for the sake of simplicity.

For unequal internal masses the singularity equations remain substantially the same, what changes are the expressions for z, z_1, and z_2. All this favors the block method over the Landau
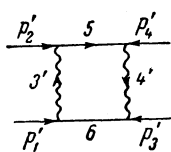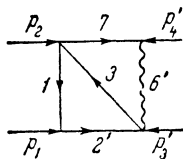
method (of course the Landau method can be applied to any diagram whereas the block method, as formulated at present, is only applicable to a definite class of diagrams), since in the latter the derivation of the one-parameter system of equations is, even in the equal-mass case, an extremely difficult problem.

The fact that we must study two equations with one parameter (in the "block" method as well as, in the end, in the Landau method) is apparently no accident and is due to the character of singularities of type C as opposed to singularities of type A or B.

The advantage of the "block" method is due to its close relation to unitarity. For the diagram of Fig. 4a the unitarity condition in channel s is three-particle and it is clear that the imaginary part of the entire diagram is given by an integral over the imaginary part of the block B_1 or B_2 (multiplied by certain other functions). This simplifies the study of absorptive parts and spectral functions of rather complicated diagrams, whose structure is like that shown in Fig. 8.

Lastly, the "block" method may be generalized to the calculation of the singularities of many-point functions of a certain class, and also to other more complicated classes of diagrams for the scattering amplitude, for example to the study of the singularities of the diagram of Fig. 3. A separate article of the authors will be devoted to these matters.

FIG. 16   FIG. 17

[1] S. Mandelstam, Phys. Rev. 112, 1344 (1958).

[2] R. Eden, Phys. Rev. 121, 1567 (1961).

[3] Karplus, Sommerfield, and Wichmann, Phys. Rev. 114, 376 (1959).

[4] Eden, Landshoff, Polkinghorne, and Taylor, J. Math. Phys. 2, 656 (1961).

[5] Kolkunov, Okun', and Rudik, JETP 38, 877 (1960), Soviet Phys. JETP 11, 634 (1960).

[6] Patashinskiĭ, Rudik, and Sudakov, JETP 40, 298 (1961), Soviet Phys. JETP 13, 201 (1961).

[7] L. D. Landau, JETP 37, 62 (1959), Soviet Phys. JETP 10, 45 (1960).

[8] R. Cutkosky, J. Math. Phys. 1, 429 (1960).

[9] J. C. Polkinghorne and G. R. Screaton, Nuovo cimento 15, 289, 925 (1960).

[10] V. N. Gribov and I. T. Dyatlov, JETP 42, 196 (1962), Soviet Phys. JETP 15, 140 (1962).

[11] V. N. Gribov and I. T. Dyatlov, JETP 42, 1268 (1962), Soviet Phys. JETP 15, 879 (1962).

[12] Karplus, Sommerfield, and Wichmann, Phys. Rev. 111, 1187 (1958).

[13] Bonnevay, Aitchison, and Dowker, Nuovo cimento 21, 1001 (1961).

[14] Yu. A. Simonov, JETP 43, 2263 (1962), Soviet Phys. JETP 16, 1599 (1963).

[15] R. W. Lardner, Nuovo cimento 19, 77 (1961).

[16] Y. S. Kim, Univ. of Maryland preprint.

[17] I. T. Drummond, University of Cambridge preprint.

[18] A. Z. Patashinskiĭ, JETP 42, 812 (1962), Soviet Phys. JETP 15, 567 (1962).